

Long-lived $2s$ state of muonic hydrogen: population and lifetime

V. P. Popov and V. N. Pomerantsev*

Institute of Nuclear Physics, Moscow State University, 119991 Moscow, Russia

Ab initio study of the density-dependent population and lifetime of the long-lived $(\mu p)_{2s}$ and the yield of $(\mu p)_{1s}$ atoms with kinetic energy 0.9 keV have been performed for the first time. The direct Coulomb $2s \rightarrow 1s$ deexcitation is proved to be the dominant quenching mechanism of the $2s$ state at kinetic energy below $2p$ threshold and explain the lifetime of the metastable $2s$ state and high-energy 0.9 keV component of $(\mu p)_{1s}$ observed at low densities. The cross sections of the elastic, Stark and Coulomb deexcitation processes have been calculated in the close-coupling approach taking into account for the first time both the closed channels and the threshold effects due to vacuum polarization shifts of the ns states. The cross sections are used as the input data in the detailed study of the atomic cascade kinetics. The theoretical predictions are compared with the known experimental data at low densities. The 40% yield of the 0.9 keV $(\mu p)_{1s}$ atoms is predicted for liquid hydrogen density.

Introduction. Exotic hydrogen-like atoms are formed in excited states and further evolution of their initial distributions in quantum numbers and kinetic energy is defined by the competition of the radiative and collisional-induced processes during the atomic cascade. Muonic hydrogen (μ^-p) is of special interest among the exotic atoms due to its simplest structure and possibility to investigate a number of problems both the exotic atom physics and bound state QED. It is well-known, that $2s$ state plays a particular role in (μ^-p) atom due to $(2s - 2p)$ Lamb shift, $E_L = 202.0$ meV, and has no analog in hadronic atoms (pionic, kaonic, etc.) in which strong interaction leads to nuclear absorption or annihilation from this state.

As it is expected, the measuring of the E_L in the so-called μp Lamb shift experiment [1] permits to determine the mean-square charge radius of the proton with a relative accuracy of 10^{-3} and results in a better test of bound-state QED. The success of this experiment depends crucially upon the population, $\epsilon_{2s}^{\text{long}}$ (per μp atom), and lifetime, τ_{2s}^{long} , of the $2s$ state at kinetic energies below E_L . This fraction is called the *long-lived* or *metastable* fraction of the $2s$ state as the Stark $2s \rightarrow 2p$ transitions are energetically forbidden and the rate of two-photon transition to the $1s$ state is negligibly small as compared with the rate of muon decay, $\lambda_\mu = 4.55 \times 10^5 \text{ s}^{-1}$. The delayed K_α X-rays induced during the collisions (see [2] and references therein) can also occur but have not been observed [3] until now.

A high-energy component of $(\mu p)_{1s}$ with kinetic energy ~ 0.9 keV was recently discovered [4, 5] from the analysis of the time-of-flight spectra (at low gas pressures $p_{H_2} = 16$ and 64 hPa) and attributed to non-radiative quenching of the long-lived $2s$ state due to the formation of the muonic molecule in a resonant $(\mu p)_{2s} + H_2$ collision and subsequent Coulomb deexcitation of the $(pp\mu)^+$ complex (see [6] and references therein). However, a theo-

retical estimation of the quenching rate in the framework of the side path model [6] gives $\sim 5 \times 10^{10} \text{ s}^{-1}$ at liquid-hydrogen atom density (LHD = $4.25 \times 10^{22} \text{ atoms/cm}^3$) that is about an order of magnitude smaller than the value $4.4_{-1.8}^{+2.1} \times 10^{11} \text{ s}^{-1}$ extracted experimentally [5].

Contrary to this assumption, in our recent paper [7] we suggested that observed collisional quenching of the metastable $2s$ state and high-energy $(\mu p)_{1s}$ component can be explained by the direct Coulomb deexcitation (CD) process,

$$(\mu^-p)_{2s} + H \rightarrow (\mu^-p)_{1s} + H, \quad (1)$$

however, the problem of the $(\mu p)_{2s}$ metastability has not been the subject of this paper.

In the present study we confirm our previous predictions [7] by the *ab initio* quantum-mechanical calculations of the cross sections for the elastic scattering, Stark transitions and CD in the framework of the improved close-coupling approach (CCA) taking for the first time into account both the closed channels and the threshold effects due to the vacuum polarization shifts of the ns states. The calculated cross sections of the above mentioned processes have been used in the detailed calculations of the atomic cascade kinetics. The population and lifetime of the metastable $2s$ state, and the yield of the hot (0.9 keV) $(\mu p)_{1s}$ component at wide densities range ($10^{-9} - 1$) LHD are predicted.

Improved close-coupling approach. The close-coupling approach has been applied [8] by the authors to describe the elastic scattering and Stark transitions in the exotic atom-hydrogen molecule collisions. Recently [7, 9, 10, 11], the unified treatment of the elastic scattering, Stark transitions and CD in the collisions of the excited exotic (muonic, pionic and antiprotonic hydrogen) atoms with hydrogen ones have been performed in the framework of the CCA. Here, we briefly remind the main assumptions and outline of the approach.

Since (μ^-p) is neutral and in the low-lying states much smaller than target molecule, the distortion of the target electron structure during collision can be neglected and moreover the exotic atom collision with the hydrogen molecule can be approximately treated as the exotic

*This work was partially supported by Russian Foundation for Basic Research, grant No. 06-02-17156.

atom-hydrogen atom scattering. These assumptions are supported in particularly by a good agreement of the experimental data [12] and our theoretical predictions [13] for the kinetic energy distribution of π^-p atoms at the instant of nuclear absorption at LHD. Further, since vacuum polarization shifts of the ns states are about two orders of magnitude more than both the fine and hyperfine splittings, the muonic atom states are described by the non-relativistic hydrogen-like wave functions with the energies of ns states shifted (due to vacuum polarization) relative to the degenerate nl states ($l \neq 0$).

Thus the total wave function of the system ($\mu p + H$) is expanded in terms of the basis states constructed as tensor products of the free muonic and hydrogen atom wave functions and angular momentum wave function of their relative motion. In the present study we use the basis sets in which both the open and closed channels are included. The coupled second order differential equations are solved numerically by the modified Numerov method. The differential and integral cross sections for individual $nl \rightarrow n'l'$ transitions have been calculated for the principal quantum number $n = 2 - 8$ and kinetic energies that are of interest in the detailed cascade calculations.

According to our study, the closed channel effects are more pronounced for the processes in the lower states ($n = 2 - 5$) at very low collision energies especially near and below $ns - np$ thresholds. Here we produce some of our results for the $2l \rightarrow 2l'$ (elastic and Stark scattering) and CD $2l \rightarrow 1s$ transitions (see figs.1, 2) where the effects of the closed channels are the most significant and extremely important for the problem of metastable $2s$ state under consideration. All presented results below $2p$ threshold and also the rates for the CD $2s, 2p \rightarrow 1s$ transitions above $2p$ threshold have been calculated for the first time.

Figures 1 and 2 show the $(\mu p)_{n=2} + H$ collisional rates, $\lambda_{nl \rightarrow n'l'} = LHD\sigma_{nl \rightarrow n'l'}v$, of the elastic and Stark scattering and CD at LHD as a function of the laboratory kinetic energy. The calculations have been performed for three variants of the basis set: the minimal basis ($n = 1, 2$), the extended basis ($n \leq n_{\max} = 7$) and (for comparison) the basis without closed channels at all. At kinetic energy below $2p$ -threshold only a few lowest partial waves contribute to the elastic $2s \rightarrow 2s$ and CD $2s \rightarrow 1s$ cross sections and, as it is seen from Fig. 1, the proper description of the collisional processes is impossible in the subspace of the open channels. The inclusion of the nearest closed $2p$ state into the basis leads to the tremendous increase both the elastic $2s \rightarrow 2s$ and CD $2s \rightarrow 1s$ rates (about 10^3 and 10^6 times, respectively). The further extension of the basis permits to achieve the convergence when the closed states of muonic hydrogen up to $n_{\max} = 7$ were included. Above $2p$ threshold the closed channel effect is practically negligible for the elastic and Stark scattering and is less pronounced than below $2p$ threshold for CD (see Fig. 2).

The results can be qualitatively explained by the different nature of the elastic/Stark scattering and CD pro-

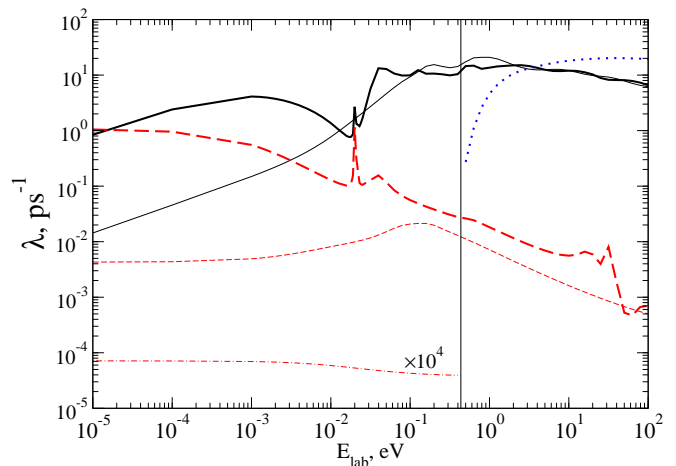


FIG. 1: Fig. 1. Collisional rates at LHD for the elastic $2s \rightarrow 2s$ scattering (solid lines), Stark $2s \rightarrow 2p$ transition (dotted line) and CD $2s \rightarrow 1s$ (dashed lines) vs. the laboratory kinetic energy. The thin lines show the results obtained with the minimal basis ($n = 1, 2$), the thick lines – with the extended basis, including all states of (μ^-p) up to $n_{\max} = 7$. For comparison the dash-dotted line shows the rate of the CD $2s \rightarrow 1s$ (multiplied by 10^4) calculated without the closed channels. The vertical line indicates the $2s - 2p$ threshold energy (0.435 eV).

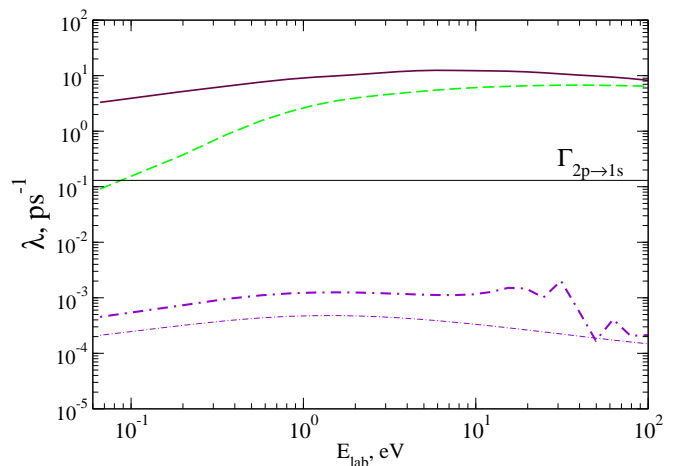


FIG. 2: Fig. 2. The same as in Fig. 1 but for the elastic $2p \rightarrow 2p$ (solid line), Stark $2p \rightarrow 2s$ (dashed line) and CD $2p \rightarrow 1s$ (dash-dotted thin and thick lines) processes. The energy is referred from $2p$ -threshold. The radiative $2p - 1s$ rate is shown with horizontal line.

cess. The elastic and Stark scattering is defined by the interaction in a range about a few atomic units (a.u.) and the high partial waves give the main contribution to the cross sections at energies above $\sim 1 - 2$ eV. So, the details of the short-range interaction (at $R < 0.1$ a.u.) are less important for description of these processes excluding the scattering at very low energies. In contrast, the CD process is accompanied by the large energy release

(tens and hundreds eV) and occurs at substantially more small distances (about a few units of the μp Bohr radius, $n^2 a_\mu$) so the details of the short-range interaction and correspondingly the closed channel effects become more important. Besides, the number of partial waves involved in the CD process is always essentially smaller than in the elastic and Stark scattering because the large centrifugal barrier for higher partial waves prevents the exotic atom from reaching the interaction range relevant for the CD process.

Since the ratios between the rates of the collisional processes are independent from the target density, the useful observations can be derived from the results presented in Figs. 1,2 without the atomic cascade calculations. The CD $2p \rightarrow 1s$ is strongly suppressed in comparison with the other cascade processes and can be neglected in the kinetics calculations. In contrast, the rate of the CD $2s \rightarrow 1s$ at kinetic energy about a few tens meV becomes comparable with the rate of the elastic $2s \rightarrow 2s$ scattering and therefore the CD $2s \rightarrow 1s$ can occur quenching the metastable $2s$ state. It is clear, the formation of the metastable $2s$ state can not lead to the fast CD $2s \rightarrow 1s$ transition before the muonic hydrogen is thermalized. Finally, the comparison of the CD $2s \rightarrow 1s$ rate with the one of muon decay permits to conclude that lifetime of the metastable $2s$ state at densities less than $\sim 10^{-6}$ LHD is mainly defined by the muon lifetime while at more higher densities the situation is quite different and the detailed kinetics calculations are needed.

Atomic cascade and the initial (n, l, E) - distributions. The cascade in the exotic atoms (see [13, 14] and references therein) is conventionally divided into classical (for $n \geq 9$) and quantum-mechanical (for $n \leq 8$) domains. In the classical domain the results of the classical-trajectory Monte Carlo calculations (for details see [14]) of the elastic scattering, Stark mixing and CD processes have been included with the molecular structure of the target taken into account. The cross sections of the external Auger effect have been calculated in the semiclassical approximation through the whole cascade. In the quantum-mechanical domain (at $n \leq 8$) the differential and integral cross sections for all $nl \rightarrow n'l'$ transitions have been calculated in the present version of the CCA.

The initial distributions in the quantum numbers (n, l) and kinetic energy E of the exotic atom at the instant of its formation are very important for the problem under consideration, especially at very low target densities relevant for the Lamb shift experiment. In the simplest picture of the exotic atom formation (usually used in the cascade calculations) the initial principal quantum number is fixed at $n_0 \sim 14$ (for muonic hydrogen) and the statistical l -distribution is assumed. More elaborate studies [15, 16, 17] taking into account the molecular structure of the target result in the initial n -distribution with the sharp peak at lower values (for muonic hydrogen at $n_0 = 11$) and non-statistical l -distribution.

Since in the limit of the lowest densities ($\lesssim 10^{-7}$ LHD) the atomic cascade is mainly defined by the muon lifetime

and the rates of the radiative transitions, the information about the initial E - and (n, l) -distributions can be obtained from the K X-ray yields and the kinetic energy distribution of muonic atoms in $1s$ state. In the present study this knowledge was used to choose the initial distribution parameters. We accept here the Gaussian distribution centered at $n_0 = 11$ as n -distribution and the modified statistical l -distribution (at each n value): $\sim (2l + 1)e^{-\alpha_l(2l+1)}$ with a one fitting parameter α_l . As for the initial kinetic energy, we use here two-exponential distribution with the parameters fitted to reproduce the integrated kinetic energy distribution of $(\mu p)_{1s}$ extracted [4] from the analysis of (μp) diffusion time at gas pressure $p_{H_2} = 0.0625$ hPa.

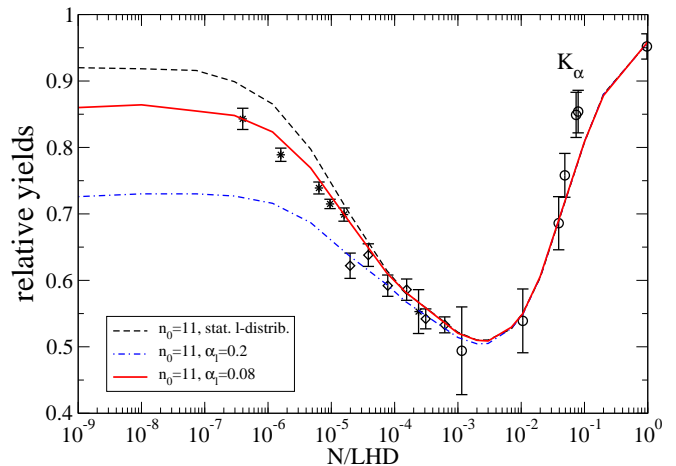


FIG. 3: Fig. 3. The density dependence of the relative K_α yield in muonic hydrogen for different variants of the initial l -distribution: statistical (dashed line) and modified statistical (solid line for $\alpha_l=0.08$ and dash-dotted line for $\alpha_l=0.1$) distributions. The experimental data are from [3] (asterisks), [18] (diamonds) and [19] (open circles).

The calculated relative K_α X-ray yields are shown in Fig. 3 in comparison with the experimental data [3, 18, 19]. The theoretical results illustrate the effect of the initial l -distribution at fixed n -distribution. It is seen that statistical l -distribution results in contradiction with the experimental data at densities $\lesssim 10^{-6}$ LHD. These differences can not be explained by the possible uncertainties in the rates of the collisional processes. Contrary to this, the modified statistical distribution ($\alpha_l=0.08$) for the first time leads as a whole to excellent agreement between theory and experimental data [3]. At densities higher than $\sim 10^{-4}$ LHD the collisional transitions and Stark mixing are more efficient and the initial l -distribution is practically forgotten during the cascade.

Metastable $2s$ fraction: population, lifetime and yield of hot $1s$ component. The population $\epsilon_{2s}^{\text{long}}$ of the metastable $2s$ state and the yield $\epsilon_{1s}^{\text{hot}}$ of the 0.9 keV $(\mu p)_{1s}$ atoms (due to CD $2s \rightarrow 1s$ below $2p$ threshold) calculated in the present version of the atomic cascade are shown in Fig. 4 for two variants of the initial l -

distribution: statistical ($\alpha_l = 0$) and modified statistical ($\alpha_l = 0.08$).

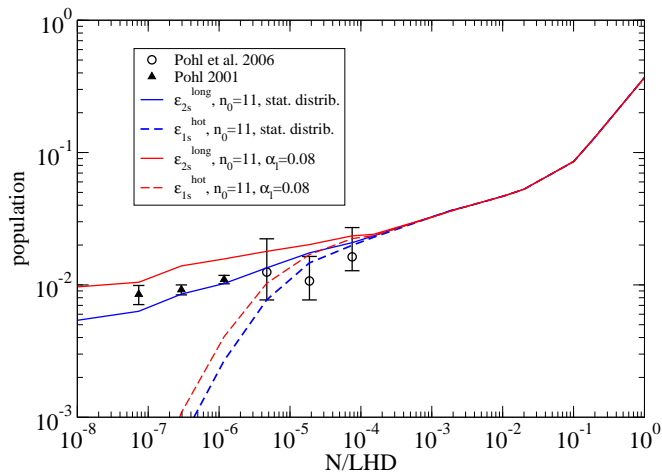


FIG. 4: Fig. 4. Density dependence of the population $\epsilon_{2s}^{\text{long}}$ (solid lines) and the yield $\epsilon_{1s}^{\text{hot}}$ (dashed lines) of 0.9 keV $(\mu p)_{1s}$ atoms obtained in *ab initio* cascade calculations with statistical (thin lines) and modified statistical ($\alpha_l = 0.08$) (thick lines) initial l -distributions. The corresponding experimental data are from [4] (filled triangles) and [5] (circles).

The calculations with the modified l -distribution predict higher populations $\epsilon_{2s}^{\text{long}}$ as compared with the ones obtained with statistical l -distribution and also with the populations derived from the experimental data analysis (for details see [4, 5]) at densities below 10^{-4} LHD. According to our study, the metastable fraction is about 1 % below 10^{-7} and slowly increases in the density range $10^{-7} - 10^{-2}$ LHD to $\sim 4\%$. Above 0.01 LHD the $\epsilon_{2s}^{\text{long}}$ grows faster reaching $\sim 40\%$ at LHD. This behavior and growth of the metastable fraction above 0.01 LHD is a consequence of the dominant role of the elastic scattering $2l \rightarrow 2l$ and Stark $2p \rightarrow 2s$ transition over the radiative $2p \rightarrow 1s$ transition (see Figs.1 and 2). It is worth noting that density dependence of the $\epsilon_{2s}^{\text{long}}$ obtained in the present study with the statistical l -distribution are similar to the one obtained earlier by Jensen and Markushin [14] only below 10^{-4} LHD. At higher densities our calculations do not confirm the sharper increase of the population up to 65% at LHD predicted in [14]. The theoretical prediction for the $\epsilon_{2s}^{\text{long}}$ is in an agreement with the experimental result [5] obtained in measurements of 0.9 keV $(\mu^- p)_{1s}$ at low gas pressures $p_{H_2} = 16$ and 64 hPa.

The calculated for the first time yields $\epsilon_{1s}^{\text{hot}}$ of the hot (0.9 keV) fraction $(\mu p)_{1s}$ (see Fig. 4) at densities below 10^{-4} LHD have a quite different density dependence as compared with the one of the $\epsilon_{2s}^{\text{long}}$. In the density range $10^{-7} - 10^{-4}$ LHD, according to our calculations, the hot fraction increases from 0.01% to $\sim 2\%$. Above 10^{-4} LHD the values of the $\epsilon_{1s}^{\text{hot}}$ and $\epsilon_{2s}^{\text{long}}$ is practically coincide. Such a behavior can be explained by the growth of the thermalized fraction of the $(\mu p)_{2s}$ atoms when the density increasing. At very low densities (below 10^{-7} LHD)

the thermalized fraction of the $(\mu p)_{2s}$ below $2p$ threshold is negligibly small and the yield of the hot fraction is less than 0.01%. At higher densities it sharply increases with the density increasing and reaches $\sim 1\%$ at 10^{-5} LHD. Above $\sim 10^{-4}$ LHD the $(\mu p)_{2s}$ atoms (below $2p$ threshold) are slowed down to low energies and then quenched in collisions by the direct $2s \rightarrow 1s$ CD and as it is demonstrated in Fig. 4 the population $\epsilon_{2s}^{\text{long}}$ and the yield of the hot fraction $\epsilon_{1s}^{\text{hot}}$ are equal to each other. According to our study, we predict that the yield of the 0.9 keV $(\mu p)_{1s}$ atoms and the yield of the protons with kinetic energy 1 keV at LHD is about $\sim 40\%$.

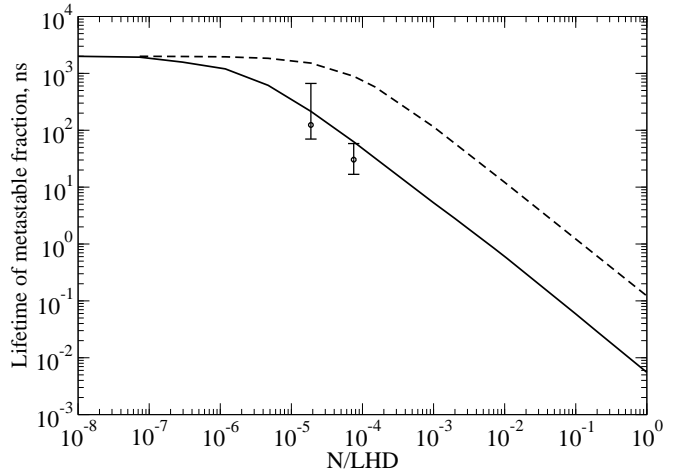


FIG. 5: Fig. 5. The density dependence of the lifetime, τ_{2s}^{long} , calculated with the extended basis set with $n_{\text{max}}=7$ (solid line) and with the minimal basis set including only closed $2p$ state (dashed line). The experimental data are from [5].

The density dependence of the lifetime τ_{2s}^{long} calculated with the extended basis set with $n_{\text{max}} = 7$ in comparison with the result obtained with the basis including only the closed $2p$ state is shown in Fig.5. The extended basis calculations are in a good agreement with the experimental data [5]. According to our study, at densities below 10^{-7} LHD the lifetime of the metastable $2s$ state is mainly determined by the muon lifetime. At the density range $10^{-7} - 10^{-5}$ LHD we observe the competition between the muon decay and the non-radiative quenching of the metastable $2s$ state due to the direct CD $2s \rightarrow 1s$. Above $10^{-5} - 10^{-4}$ LHD the quenching of the long-lived $2s$ state is entirely determined by the CD process.

Conclusion. For the first time the cross sections for the $(\mu p) + H$ scattering process – elastic, Stark and Coulomb deexcitation – are calculated in the close-coupling approach *including the closed channels*. These cross sections are used as the input data for detailed study of the atomic cascade kinetics in wide density range ($10^{-9} - 1$) LHD. The results of our treatment allow us to assert that the direct Coulomb $2s \rightarrow 1s$ deexcitation (calculated for the first time both above and below $2s-2p$ threshold) is the *dominant quenching mechanism* of the long-lived $2s$ fraction and explains the experimental value

of its lifetime. The calculated population and lifetime of the metastable $2s$ -state and also predicted yield of the hot component $(\mu p)_{1s}$ with kinetic energy ~ 0.9 keV can be very useful for the choice of the optimal conditions for the μp Lamb shift experiment and other experiments. In particular, it will be very interesting to obtain experimental data about the density dependence of the yield of the hot component $(\mu p)_{1s}$ with kinetic energy ~ 0.9 keV

or the yield of the protons with kinetic energy 1 keV.

Acknowledgments. We thank L. Simons for permanent interest in our studies and fruitful discussions; T. Jensen for the fruitful cooperation in the development of the new version of the cascade code; L. Ponomarev and the participants of the Seminar in MUCATEX for useful discussions. This work was supported by Russian Foundation for Basic Research (grant No. 06-02-17156).

-
- [1] R. Pohl, A. Antognini, F.D. Amaro et al., *Can. J. Phys.* **83**, 339 (2005).
- [2] L.I. Men'shikov and L.I. Ponomarev, *Z. Phys. D* **2**, 1 (1986).
- [3] H. Anderhub, H.P. von Arb, J. Böcklin et al., *Phys. Lett. B* **143**, 65 (1984).
- [4] R. Pohl, Ph.D. thesis 14096, ETH Zurich, 2001.
- [5] R. Pohl, H. Daniel, F.J. Hartmann et al., *PRL* **97**, 193402 (2006).
- [6] J. Wallenius, S. Jonsell, Y. Kino and P. Froelich, *Hyperfine Interact.* **138**, 285 (2001).
- [7] V.N. Pomerantsev and V.P. Popov, *JETP Lett.* **83**, 331 (2006).
- [8] V.P. Popov and V.N. Pomerantsev, *Hyperfine Interact.* **138**, 109 (2001).
- [9] G.Ya. Korenman, V.N. Pomerantsev, and V.P. Popov, *JETP Lett.* **81**, 543 (2005); nucl-th/0501036.
- [10] V.N. Pomerantsev and V.P. Popov, *Phys. Rev. A* **73**, 040501(R) (2006).
- [11] V.P. Popov and V.N. Pomerantsev, arXiv:0712.3111.
- [12] A. Badertscher, M. Daum, P.F.A. Goudsmit et al., *Europhys. Lett.* **54**, 313 (2001).
- [13] T.S. Jensen, V.P. Popov and V.P. Pomerantsev, arXiv:0712.3010.
- [14] T.S. Jensen and V.E. Markushin, *Eur. Phys. J. D* **21**, 271 (2002).
- [15] G.Ya. Korenman and V.P. Popov, *Muon Catalyzed Fusion* **4**, 145 (1989).
- [16] G.Ya. Korenman, V.P. Popov and G.A. Fesenko, *Muon Catalyzed Fusion* **7**, 179 (1992).
- [17] J.S. Cohen, *Rep.Prog. Phys.* **67** (2004) 1769.
- [18] N. Bregant, D. Chatellard, J.P. Egger et al., *Phys. Lett. A* **241**, 344 (1998).
- [19] B. Lauss, P. Ackebauer, W.H. Breunlich et al., *Phys. Rev. Lett.* **80**, 3041 (1998).